Northumbria Research Link

Citation: Vo, Thuc and Thai, Huu-Tai (2012) Static behavior of composite beams using various refined shear deformation theories. Composite Structures, 94 (8). 2513 - 2522. ISSN 0263-8223

Published by: Elsevier

URL: http://dx.doi.org/10.1016/j.compstruct.2012.02.010 <http://dx.doi.org/10.1016/j.compstruct.2012.02.010>

This version was downloaded from Northumbria Research Link: http://nrl.northumbria.ac.uk/id/eprint/13386/

Northumbria University has developed Northumbria Research Link (NRL) to enable users to access the University's research output. Copyright © and moral rights for items on NRL are retained by the individual author(s) and/or other copyright owners. Single copies of full items can be reproduced, displayed or performed, and given to third parties in any format or medium for personal research or study, educational, or not-for-profit purposes without prior permission or charge, provided the authors, title and full bibliographic details are given, as well as a hyperlink and/or URL to the original metadata page. The content must not be changed in any way. Full items must not be sold commercially in any format or medium without formal permission of the copyright holder. The full policy is available online: http://nrl.northumbria.ac.uk/policies.html

This document may differ from the final, published version of the research and has been made available online in accordance with publisher policies. To read and/or cite from the published version of the research, please visit the publisher's website (a subscription may be required.)

Northumbria University NEWCASTLE

CUSTOMER SERVICE EXCELLENCE CSE UniversityLibrary

*Manuscript without line numbers
Click here to view linked References

Static behaviour of composite beams using various refined shear deformation theories

Thuc P. Vo[a,b,*], Huu-Tai Thai[c]

[a] *School of Mechanical, Aeronautical and Electrical Engineering, Glyndŵr University, Mold Road, Wrexham LL11 2AW, UK.*
[b] *Advanced Composite Training and Development Centre, Unit 5, Hawarden Industrial Park Deeside, Flintshire CH5 3US, UK.*
[c] *Department of Civil and Environmental Engineering, Hanyang University, 17 Haengdang-dong, Seongdong-gu, Seoul 133-791, Republic of Korea.*

Abstract

Static behaviour of composite beams with arbitrary lay-ups using various refined shear deformation theories is presented. The developed theories, which do not require shear correction factor, account for parabolical variation of shear strains and consequently shear stresses through the depth of the beam. In addition, they have strong similarity with Euler-Bernoulli beam theory in some aspects such as governing equations, boundary conditions, and stress resultant expressions. A two-noded C^1 finite element with six degree-of-freedom per node which accounts for shear deformation effects and all coupling coming from the material anisotropy is developed to solve the problem. Numerical results are performed for symmetric and anti-symmetric cross-ply composite beams under the uniformly distributed load and concentrated load. The effects of fiber angle and lay-ups on the shear deformation parameter and extension-bending-shear-torsion response are investigated.

Keywords: Composite beams; higher-order theory; shear deformation parameter ; fourfold coupled response.

1. Introduction

Composite materials are increasingly being used in various engineering applications due to their attractive properties in strength, stiffness, and lightness. Finite element models originally developed for one-layered isotropic structures were extended to laminated composite structures as equivalent single-layer (ESL) models. These models are known to provide a sufficiently accurate description of the global response of thin to moderately thick laminates [1] and considered in this paper. In company with the increase in the application of composite materials in engineering structures, many beam theories have

*Corresponding author, tel.: +44 1978 293979
Email address: t.vo@glyndwr.ac.uk (Thuc P. Vo)

been developed for predicting the response of laminated composite beams. A review of different beam theories for the analysis of isotropic and laminated beams was presented by Ghugal and Shimpi [2]. Assessments of several beam theories were performed by Aguiar et al. [3] and Zhen and Wanji [4] for static, vibration, and stability analyses of composite beams. According to Ghugal and Shimpi [2], all of these beam theories can be classified into three main categories: the classical beam theory (CBT), the first-order beam theory (FOBT) and the higher-order beam theory (HOBT). The CBT known as Euler-Bernoulli beam theory is the simplest one and is applicable to slender beams only. For moderately deep beams, it underestimates deflection and overestimates buckling load and natural frequency due to ignoring the transverse shear effects ([5]-[7]). The FOBT known as Timoshenko beam theory is proposed to overcome the limitations of the CBT by accounting for the transverse shear effects. Since the FOBT violates the zero shear stress conditions on the top and bottom surfaces of the beam, a shear correction factor is required to account for the discrepancy between the actual stress state and the assumed constant stress state. To remove the discrepancies in the CBT and FOBT, the HOBTs are developed to avoid the use of shear correction factor and have a better prediction of response of laminated beams. The HOBTs can be developed based on the assumption of the higher-order variation of in-plane displacement ([8]-[12]) or both in-plane and transverse displacements ([13]-[20]) through the depth of the beam. There is another type of higher-order theories which use trigonometric, hyperbolic and exponential functions to represent the shear deformation effects. By using these higher-order theories, although several authors have investigated the static, vibration and buckling behaviour of composite plates ([21]-[26]), the existing literature reveals that studies of flexural analysis of composite beams with arbitrary lay-ups are limited. Although the HOBTs offer a slight improvement in accuracy compared to the FOBT, they are computationally more demanding due to higher-order terms included in the theories. Hence, there is a scope to develop accurate refined shear deformation beam theories which are simple to use to solve the problem.

In this paper, various refined shear deformation beam models are presented to study the static responses of composite beams with arbitrary lay-ups under vertical loads. The displacement fields of the present theories are chosen based on the following assumptions: (1) the axial and transverse displacements consist of bending and shear components in which the bending components do not contribute toward shear forces and, likewise, the shear components do not contribute toward bending moments; (2) the bending component of axial displacement is similar to that given by the CBT; and (3) the shear component of axial displacement gives rise to the higher-order variation of shear strain and hence to shear stress through the depth of the beam in such a way that shear stress vanishes on the top and bottom surfaces. The most interesting feature of these beam models is that

it satisfies the zero traction boundary conditions on the top and bottom surfaces of the beam without using shear correction factors. The governing equations are derived from the principle of virtual displacements. A two-noded C^1 finite element with six degree-of-freedom per node which accounts for shear deformation effects and all coupling coming from the material anisotropy is developed to solve the problem. Numerical results are performed for symmetric and anti-symmetric cross-ply composite beams under the uniformly distributed load and concentrated load. The effects of fiber angle and lay-ups on the shear deformation parameter and extension-bending-shear-torsion response are investigated.

2. Kinematics

A laminated composite beam made of many plies of orthotropic materials in different orientations with respect to the x-axis, as shown in Fig. 1, is considered. For generality purpose, the displacement field in the beam is assumed to be:

$$U(x,z) = u(x) - z\frac{\partial w_b(x)}{\partial x} - f(z)\frac{\partial w_s(x)}{\partial x} \tag{1a}$$

$$V(x,z) = z\phi(x) \tag{1b}$$

$$W(x,z) = w_b(x) + w_s(x) \tag{1c}$$

where u is the axial displacement along the mid-plane of the beam, w_b and w_s are the bending and shear components of transverse displacement along the mid-plane of the beam, ϕ is rotation of the normal to the mid-plane about x-axis and $f(z)$ represents shape function determining the distribution of the transverse shear strains and stress through the depth of the beam. Eq. (1) contains the displacement field of the CBT, FOBT, HOBT based on Reddy [27] and the sinusoidal shear beam theory (SSBT) based on Touratier [21]. Each displacement field can be obtained by using the function $f(z)$ given in Table 1.

The non-zero strains are given by:

$$\epsilon_x = \frac{\partial u}{\partial x} = \epsilon_x^\circ + z\kappa_x^b + f\kappa_x^s \tag{2a}$$

$$\gamma_{xz} = \frac{\partial w}{\partial x} + \frac{\partial u}{\partial z} = (1-f')\gamma_{xz}^\circ = g\gamma_{xz}^\circ \tag{2b}$$

$$\gamma_{xy} = \frac{\partial u}{\partial y} + \frac{\partial v}{\partial x} = z\kappa_{xy} \tag{2c}$$

where $\epsilon_x^\circ, \gamma_{xz}^\circ, \kappa_x^b, \kappa_x^s$ and κ_{xy} are axial strain, shear strains and curvatures in the beam, respectively

defined as:

$$\epsilon_x^\circ = u' \tag{3a}$$

$$\gamma_{xz}^\circ = w_s' \tag{3b}$$

$$\kappa_x^b = -w_b'' \tag{3c}$$

$$\kappa_x^s = -w_s'' \tag{3d}$$

$$\kappa_{xy} = \phi' \tag{3e}$$

where differentiation with respect to the x-axis is denoted by primes ($'$).

3. Variational Formulation

Total potential energy of the system is calculated by sum of strain energy and the work done by external forces:

$$\Pi = \mathcal{U} + \mathcal{V} \tag{4}$$

where $\mathcal{U}$ is the strain energy:

$$\mathcal{U} = \frac{1}{2}\int_v (\sigma_x \epsilon_x + \sigma_{xz}\gamma_{xz} + \sigma_{xy}\gamma_{xy}) dv \tag{5}$$

The strain energy is calculated by substituting Eq. (2) into Eq. (5):

$$\mathcal{U} = \frac{1}{2}\int_v \Big[\sigma_x(\epsilon_x^\circ + z\kappa_x^b + f\kappa_x^s) + \sigma_{xz} g\gamma_{xz}^\circ + \sigma_{xy} z\kappa_{xy}\Big] dv \tag{6}$$

The variation of the strain energy can be stated as:

$$\delta\mathcal{U} = \int_0^l (N_x \delta\epsilon_z^\circ + M_x^b \delta\kappa_x^b + M_x^s \delta\kappa_x^s + Q_{xz}\delta\gamma_{xz}^\circ + M_{xy}\delta\kappa_{xy}) dx \tag{7}$$

where $N_x, M_x^b, M_x^s, Q_{xz}$ and M_{xy} are the axial force, bending moments, shear force and torsional moment, respectively, defined by integrating over the cross-sectional area A as:

$$N_x = \int_A \sigma_x dA \tag{8a}$$

$$M_x^b = \int_A \sigma_x z dA \tag{8b}$$

$$M_x^s = \int_A \sigma_x f dA \tag{8c}$$

$$Q_{xz} = \int_A \sigma_{xz} g dA \tag{8d}$$

$$M_{xy} = \int_A \sigma_{xy} z dA \tag{8e}$$

On the other hand, the variation of work done by external forces can be written as:

$$\delta\mathcal{V} = -\int_0^l \left[\mathcal{P}_x\delta u + \mathcal{P}_z(\delta w_b + \delta w_s)\right]dx \tag{9}$$

Principle of total potential energy can be stated as:

$$0 = \delta\Pi = \delta\mathcal{U} + \delta\mathcal{V} \tag{10}$$

The weak form of the HOBT and SSBT for composite beams is given by substituting Eqs. (7) and (9) into Eq. (10):

$$0 = \int_0^l \Big[N_z\delta u' - M_x^b\delta w_b'' - M_x^s\delta w_s'' + M_{xy}\delta\phi' + Q_{xz}\delta w_s' - \mathcal{P}_x\delta u - \mathcal{P}_z(\delta w_b + \delta w_s)\Big]dx \tag{11}$$

Due to the absence of function $f(z)$ in Eq. (8c), the weak form of the FOBT becomes:

$$0 = \int_0^l \Big[N_z\delta u' - M_x^b\delta w_b'' + M_{xy}\delta\phi' + Q_{xz}\delta w_s' - \mathcal{P}_x\delta u - \mathcal{P}_z(\delta w_b + \delta w_s)\Big]dx \tag{12}$$

4. Constitutive Equations

The constitutive equations of a k^{th} orthotropic lamina in the laminate co-ordinate system of section are given by:

$$\left\{\begin{array}{c}\sigma_x\\ \sigma_{xy}\end{array}\right\}^k = \left[\begin{array}{cc}\bar{Q}_{11}^* & \bar{Q}_{16}^*\\ \bar{Q}_{16}^* & \bar{Q}_{66}^*\end{array}\right]^k \left\{\begin{array}{c}\epsilon_x\\ \gamma_{xy}\end{array}\right\} \tag{13}$$

where $\bar{Q}_{ij}^*$ are transformed reduced stiffnesses and can be calculated from the transformed stiffnesses based on the plane stress and plane strain assumption. More detailed explanation can be found in Ref. [28].

The constitutive relation for out-of-plane stress and strain is given by:

$$\sigma_{xz} = \bar{Q}_{55}\gamma_{xz} \tag{14}$$

The constitutive equations for bar forces and bar strains are obtained by using Eqs. (2), (8), (13) and (14):

$$\left\{\begin{array}{c}N_x\\ M_x^b\\ M_x^s\\ M_{xy}\\ Q_{xz}\end{array}\right\} = \left[\begin{array}{ccccc}R_{11} & R_{12} & R_{13} & R_{14} & 0\\ & R_{22} & R_{23} & R_{24} & 0\\ & & R_{33} & R_{34} & 0\\ & & & R_{44} & 0\\ \text{sym.} & & & & R_{55}\end{array}\right] \left\{\begin{array}{c}\epsilon_x^\circ\\ \kappa_x^b\\ \kappa_x^s\\ \kappa_{xy}\\ \gamma_{xz}^\circ\end{array}\right\} \tag{15}$$

where R_{ij} are the laminate stiffnesses of general composite beams and given by:

$$R_{11} = \int_A \bar{Q}^*_{11} dA \tag{16a}$$

$$R_{12} = \int_A \bar{Q}^*_{11} z dA \tag{16b}$$

$$R_{13} = \int_A \bar{Q}^*_{11} f dA \tag{16c}$$

$$R_{14} = \int_A \bar{Q}^*_{16} z dA \tag{16d}$$

$$R_{22} = \int_A \bar{Q}^*_{11} z^2 dA \tag{16e}$$

$$R_{23} = \int_A \bar{Q}^*_{11} f z dA \tag{16f}$$

$$R_{24} = \int_A \bar{Q}^*_{16} z^2 dA \tag{16g}$$

$$R_{33} = \int_A \bar{Q}^*_{11} f^2 dA \tag{16h}$$

$$R_{34} = \int_A \bar{Q}^*_{16} f z dA \tag{16i}$$

$$R_{44} = \int_A \bar{Q}^*_{66} z^2 dA \tag{16j}$$

$$R_{55} = \int_A \bar{Q}_{55} g^2 dA \tag{16k}$$

It is from Eq. (16) that the difference between each theory can be found in the laminate stiffnesses terms dealing with functions $f(z)$ and $g(z)$ as indicated in Table 1, these terms are $R_{i,3}, i = 1..4$ and R_{55}. The explicit of the laminate stiffnesses for each theory is given in Appendix A.

5. Governing Equations

The equilibrium equations of the present study can be obtained by integrating the derivatives of the varied quantities by parts and collecting the coefficients of $\delta u, \delta w_b, \delta w_s$ and $\delta\phi$:

$$N'_x + \mathcal{P}_x = 0 \tag{17a}$$

$$M^{b\prime\prime}_x + \mathcal{P}_z = 0 \tag{17b}$$

$$M^{s\prime\prime}_x - Q'_{xz} + \mathcal{P}_z = 0 \tag{17c}$$

$$M'_{xy} = 0 \tag{17d}$$

The natural boundary conditions are of the form:

$$\delta u \ : \ N_x \tag{18a}$$

$$\delta w_b \;:\; M_x^{b\prime} \tag{18b}$$

$$\delta w_b' \;:\; M_x^{b} \tag{18c}$$

$$\delta w_s \;:\; M_x^{s\prime} + Q_{xz} \tag{18d}$$

$$\delta w_s' \;:\; M_x^{s} \tag{18e}$$

$$\delta \phi \;:\; M_{xy} \tag{18f}$$

By substituting Eqs. (3) and (15) into Eq. (17), the explicit form of the governing equations can be expressed with respect to the laminate stiffnesses R_{ij}:

$$R_{11}u'' - R_{12}w_b''' - R_{13}w_s''' + R_{14}\phi'' + \mathcal{P}_x = 0 \tag{19a}$$

$$R_{12}u''' - R_{22}w_b^{iv} - R_{23}w_s^{iv} + R_{24}\phi''' + \mathcal{P}_z = 0 \tag{19b}$$

$$R_{13}u''' - R_{23}w_b^{iv} - R_{33}w_s^{iv} + R_{34}\phi''' - R_{55}w_s'' + \mathcal{P}_z = 0 \tag{19c}$$

$$R_{14}u'' - R_{24}w_b''' - R_{34}w_s''' + R_{44}\phi'' = 0 \tag{19d}$$

Eq. (19) is the most general equilibrium equations for the extension, bending, shear and torsion behaviour of composite beams under various types of loadings, and the dependent variables, u, w_b, w_s and ϕ are fully coupled.

6. Finite Element Formulation

The present theory for composite beams described in the previous section was implemented via a displacement based finite element method.

6.1. Interpolation function for the HOBT and SSBT

The variational statement in Eq. (11) requires that the bending and shear components of transverse displacement w_b and w_s be twice differentiable and C^1-continuous, whereas the axial displacement u and rotation ϕ must be only once differentiable and C^0-continuous. The generalized displacements are expressed over each element as a combination of the linear interpolation function Ψ_j for u and ϕ and Hermite-cubic interpolation function ψ_j for w_b and w_s associated with node j and the nodal values:

$$u = \sum_{j=1}^{2} u_j \Psi_j \tag{20a}$$

$$w_b = \sum_{j=1}^{4} w_{bj} \psi_j \tag{20b}$$

$$w_s = \sum_{j=1}^{4} w_{sj}\psi_j \tag{20c}$$

$$\phi = \sum_{j=1}^{2} \phi_j \Psi_j \tag{20d}$$

6.2. Interpolation function for the FOBT

The variational statement in Eq. (12) requires that bending component displacement w_b be twice differentiable and C^1-continuous, whereas the axial displacement u, the shear component displacement w_s and rotation ϕ must be only once differentiable and C^0-continuous. The generalized displacements are expressed over each element as a combination of the linear interpolation function Ψ_j for u, w_s and ϕ and Hermite-cubic interpolation function ψ_j for w_b associated with node j and the nodal values:

$$u = \sum_{j=1}^{2} u_j \Psi_j \tag{21a}$$

$$w_b = \sum_{j=1}^{4} w_{bj}\psi_j \tag{21b}$$

$$w_s = \sum_{j=1}^{2} w_{sj}\Psi_j \tag{21c}$$

$$\phi = \sum_{j=1}^{2} \phi_j \Psi_j \tag{21d}$$

Substituting these expressions in Eqs. (20) and (21) into the corresponding weak statement in Eqs. (11) and (12), the finite element model of a typical element can be expressed as:

$$\begin{bmatrix} K_{11} & K_{12} & K_{13} & K_{14} \\ & K_{22} & K_{23} & K_{24} \\ & & K_{33} & K_{34} \\ \text{sym.} & & & K_{44} \end{bmatrix} \begin{Bmatrix} u \\ w_b \\ w_s \\ \phi \end{Bmatrix} = \begin{Bmatrix} F_1 \\ F_2 \\ F_3 \\ F_4 \end{Bmatrix} \tag{22a}$$

where $[K]$ is the element stiffness matrix and $[F]$ is the element force vector. The explicit of them is given in the Appendix B.

It is clear that for the HOBT and SSBT, a two-noded C^1 finite element with six degree-of-freedom per node is used, while five degree-of-freedom per node is used for the FOBT. Besides, since C^1 finite element is used, the shear locking can be avoided for the FOBT.

7. Numerical Examples

For verification purpose, a number of numerical examples are presented and analysed using different theory (CBT, FOBT, HOBT and SSBT). In the case of the FOBT, a value of 5/6 is used for the shear correction factor. A cantilever isotropic beam under an end load P and a simply-supported isotropic beam under a uniform load q are considered first. The exact solutions [29] for the maximum displacements for these two cases, when using the higher-order theory, are given by:

$$w^c = \frac{1}{3}\frac{PL^3}{EI} + \frac{1}{5}\frac{PL^3}{EI}(1+\nu)\frac{h}{L^2}(1 - \frac{1}{\lambda L}\tanh\lambda L), \quad \lambda = \frac{420}{(1+\nu)h} \tag{23a}$$

$$w^{ss} = \frac{5}{384}\frac{qL^4}{EI} + \frac{5}{24}\frac{qL^4}{EI}\Big[\frac{3}{25}(1+\nu)\frac{h}{L^2} - \frac{2}{875}(1+\nu)^2\frac{h}{L^4}\Big] \tag{23b}$$

where the superscripts c and ss represent the cantilever and simply-supported beam solutions, respectively. The material and geometric properties are $E = 29000, \nu = 0.3, b = 1, P = 100$ and $q = 10$. These problems are solved here to compare with other theories for several span-to-height L/h ratios. The maximum displacements are calculated and given in Table 2, with the previous finite elements results ([12], [30], [31] and [32]) and Euler, Timoshenko theory results [31]. The current results are in excellent agreement with other researchers and the exact solutions for both cases.

In the next example, a cantilever unidirectional composite beam with $L/h = 9$ is performed for two load cases: a uniformly distributed load, and a concentrated tip load (Fig. 2). The material properties and loading cases are given in Table 3. The vertical displacements at the free end are given in Table 4 with the previous result obtained based on the FOBT of Lin and Zhang [32] and Davalos et al. [33] and the HOBT of Surana and Nguyen [34]. The table shows an excellent agreement between the predictions of the present model and the results of the other models mentioned.

To demonstrate the accuracy and validity of this study further, symmetric $[0°/90°/0°]$ and anti-symmetric cross-ply $[0°/90°]$ composite beams under a uniformly distributed load are analysed. Beams with cantilever and simply supported boundary conditions are considered. All laminate in the present study are of equal thickness and made of the same orthotropic material, whose properties are:

$$E_1/E_2 = 25, G_{12} = G_{13} = 0.5E_2, G_{23} = 0.2E_2, \nu_{12} = 0.25 \tag{24}$$

For convenience, the following non-dimensional terms are used, the vertical displacement and in-plane and transverse shear stresses of beams under the uniformly distributed load q:

$$\overline{w} = \frac{wbhE_2h^2 10^2}{qL^4} \tag{25a}$$

$$\overline{\sigma}_x = \frac{bh^2}{qL^2}\sigma_x(L/2, h/2) \tag{25b}$$

$$\overline{\sigma}_{xz} = \frac{bh}{qL}\sigma_{xz}(0,0) \tag{25c}$$

and the axial, vertical and torsional displacements of beams under the concentrated tip load P:

$$\overline{u} = \frac{ubhE_2}{PL} \tag{26a}$$

$$\overline{w} = \frac{wbhE_2h^2}{PL^3} \tag{26b}$$

$$\overline{\phi} = \frac{\phi bhG_{12}h^2}{PL^2} \tag{26c}$$

as well as a parameter α is defined to assess the effect of shear deformation:

$$\alpha = \frac{w_s}{w} \tag{27}$$

The mid-span displacements for different L/h ratios are compared with exact solutions [7] and the finite elements results ([3], [12], [18], [35]) in Tables 5 and 6. Effect of span-to-height ratio on in-plane and transverse shear stresses of a simply-supported composite beam is given in Table 7. Distribution of these stresses through-the-thickness for $L/h = 5$ is also plotted in Figs. 3 and 4. An excellent agreement between present models and the corresponding previous results, for each theory can be observed. It can be noticed that displacements obtained from the HOBT and SSBT are very close in all examples in present study. This is due simply to the form of function $f(z)$ which in the case of the HOBT corresponds to a development in series up to the order 3 of function sin in the SSBT. The shear deformation parameter with respect to span-to-height ratio obtained by using the FOBT, HOBT and SSBT is plotted in Figs. 5 and 6. This parameter depends not only on the span-to-height ratio but also lay-up. It is clear that shear effect on symmetric cross-ply is more pronounced than anti-symmetric one for a given span-to-height ratio. For symmetric cross-ply, the shear theories become very effective in a relatively large region up to the point where span-to-height ratio reaches value of $L/h = 25$. The shear deformation parameter increases in the order FOBT, HOBT and SSBT. It indicates that only the last two theories are capable of revealing exactly the influence of shear deformation, especially for lower span-to-height ratio.

The next example shows the effects of fiber orientation on the vertical displacements of simply supported anti-symmetric angle-ply $[\theta/-\theta]_2$ composite beams with $L/h = 5$ and $L/h = 10$ under the uniformly distributed load. Variation of the bending and shear components of vertical displacement at mid-span with respect to the fiber angle change using different theory is shown in Figs. 7 and 8. As expected, the bending and shear components obtained using the HOBT and SSBT are nearly identical. The bending component obtained using the SSBT is the smallest, whereas the shear one is the largest. As the fiber angle increases, the bending components increase more rapidly than the shear ones. It is clear that the shear effect is negligible in this lay-up even for $L/h = 10$ (Fig. 8). When using the HOBT, the orthotropy solution or uncoupled solution, which neglects the coupling effects coming from

the material anisotropy, are also given. Variation of the maximum vertical displacements at mid-span of the beam with respect to the fiber angle change is shown in Fig. 9. For this stacking sequence, the coupling stiffness R_{14} and R_{23} do not vanish while all the other coupling stiffnesses become zero. That is, the orthotropy solution might not be accurate. However, since the coupling stiffness is small, the coupling effects coming from the material anisotropy become negligible. Consequently, the present solution and the orthotropy solution agrees well as shown in Fig. 9. It is indicated that the orthotropy solution is sufficiently accurate for this lay-up.

In order to investigate the coupling and shear effects further on the axial-flexural-torsional response, cantilever $[0^\circ/\theta]_2$ composite beams with $L/h = 5$ and $L/h = 10$ under the concentrated tip load are analysed using the HOBT. For this lay-up, the coupling stiffnesses $R_{12}, R_{13}, R_{14}, R_{23}$ and R_{24} do not vanish. Variation of the vertical displacements at mid-span with respect to the fiber angle change is shown in Fig. 10. The finite element solution using the CBT is also displayed. The solution excluding shear effect remarkably underestimates the displacement for all the range of the fiber angle. As the fiber angle increases, the orthotropy solution disagree with the finite element solution as anisotropy of the beam gets higher. Variation of the axial and torsional displacements at mid-span with respect to fiber angle change is shown in Figs. 11 and 12. It is clear that the angle of twist is not affected by shear effect since its value is identical for both $L/h = 5$ and $L/h = 10$. The maximum angle of twist occurs near $\theta = 20^\circ$, that is, because the torsional rigidity E_{44} becomes maximum value at this value. It is from Figs. 11 and 12 that highlight the influence of coupling effects on the axial displacement and angle of twist of the beam. These responses are never seen in isotropic material because the coupling terms are not present. It implies that the structure under vertical load not only causes transverse displacement as would be observed in isotropic material, but also causes additional responses due solely to coupling effects. That is, the orthotropy solution is no longer valid for unsymmetrically laminated beams, and and fourfold coupled extension-bending-shear-torsion equations should be considered simultaneously for accurate analysis of composite beams.

8. Conclusions

A two-noded C^1 finite element model with six degree-of-freedom per node which accounts for shear deformation effects and anisotropy coupling is developed to study the static behaviour of composite beams with arbitrary lay-ups under vertical loads. This model is capable of predicting accurately static responses for various configuration including boundary conditions, span-to-height ratio and laminate orientation. It accounts for parabolical variation of shear strains through the depth of the beam, and satisfies the zero traction boundary conditions on the top and bottom surfaces of the beam

without using shear correction factor. The orthotropy solution is accurate for lower degrees of material anisotropy, but, becomes inappropriate as the anisotropy of the beam gets higher, and fully coupled equations should be considered for accurate analysis of composite beams. The present model is found to be appropriate and efficient in analysing static problem of composite beams.

9. Appendix A

The laminate stiffnesses of composite beams in the present study can be divided by the common terms for all theories and specific terms for each theory. The common terms for all theories can be expressed by:

$$R_{11} = \int_y A_{11} dy \tag{28a}$$

$$R_{12} = \int_y B_{11} dy \tag{28b}$$

$$R_{14} = \int_y B_{16} dy \tag{28c}$$

$$R_{22} = \int_y D_{11} dy \tag{28d}$$

$$R_{24} = \int_y D_{16} dy \tag{28e}$$

$$R_{44} = \int_y D_{66} dy \tag{28f}$$

The specific terms for the FOBT can be expressed by:

$$R_{13} = R_{23} = R_{33} = R_{34} = 0 \tag{29a}$$

$$R_{55} = \int_y A_{55} dy \tag{29b}$$

The specific terms for the HOBT can be expressed by:

$$R_{13} = \int_y \frac{4}{3h^2} E_{11} dy \tag{30a}$$

$$R_{23} = \int_y \frac{4}{3h^2} F_{11} dy \tag{30b}$$

$$R_{33} = \int_y \frac{16}{9h^4} H_{11} dy \tag{30c}$$

$$R_{34} = \int_y \frac{4}{3h^2} F_{16} dy \tag{30d}$$

$$R_{55} = \int_y (A_{55} - \frac{8}{h^2} D_{55} + \frac{16}{h^4} F_{55}) dy \tag{30e}$$

The specific terms for the SSBT can be expressed by:

$$R_{13} = \int_y (B_{11} - \frac{h}{\pi} E^s_{11}) dy \tag{31a}$$

$$R_{23} = \int_y (D_{11} - \frac{h}{\pi} F^s_{11}) dy \tag{31b}$$

$$R_{33} = \int_y \left[D_{11} - 2\frac{h}{\pi} F^s_{11} + (\frac{h}{\pi})^2 G^s_{11} \right] dy \tag{31c}$$

$$R_{34} = \int_y (D_{16} - \frac{h}{\pi} F^s_{16}) dy \tag{31d}$$

$$R_{55} = \int_y H^s_{55} dy \tag{31e}$$

where A_{ij}, B_{ij} and D_{ij} matrices are extensional, coupling and bending stiffness as well as $E_{ij}, F_{ij}, G_{ij}, H_{ij}$ and $E^s_{ij}, F^s_{ij}, G^s_{ij}, H^s_{ij}$ matrices are higher order stiffnesses, respectively, defined by:

$$(A_{ij}, B_{ij}, D_{ij}, E_{ij}, F_{ij}, G_{ij}, H_{ij}) = \int \bar{Q}_{ij} (1, z, z^2, z^3, z^4, z^5, z^6) dz \tag{32a}$$

$$(E^s_{ij}, F^s_{ij}, G^s_{ij}, H^s_{ij}) = \int \bar{Q}_{ij} \Big[\sin(\frac{\pi z}{h}), z \sin(\frac{\pi z}{h}), \sin^2(\frac{\pi z}{h}), \cos^2(\frac{\pi z}{h}) \Big] dz \tag{32b}$$

10. Appendix B

The element stiffness matrix for the HOBT and SSBT is given by:

$$K^{11}_{ij} = \int_0^l R_{11} \Psi'_i \Psi'_j dz \tag{33a}$$

$$K^{12}_{ij} = -\int_0^l R_{12} \Psi'_i \psi''_j dz \tag{33b}$$

$$K^{13}_{ij} = -\int_0^l R_{13} \Psi'_i \psi''_j dz \tag{33c}$$

$$K^{14}_{ij} = \int_0^l R_{14} \Psi'_i \Psi'_j dz \tag{33d}$$

$$K^{22}_{ij} = \int_0^l R_{22} \psi''_i \psi''_j dz \tag{33e}$$

$$K^{23}_{ij} = \int_0^l R_{23} \psi''_i \psi''_j dz \tag{33f}$$

$$K^{24}_{ij} = -\int_0^l R_{24} \psi''_i \Psi'_j dz \tag{33g}$$

$$K^{33}_{ij} = \int_0^l (R_{33} \psi''_i \psi''_j + R_{55} \psi'_i \psi'_j) dz \tag{33h}$$

$$K^{34}_{ij} = -\int_0^l R_{34} \psi''_i \Psi'_j dz \tag{33i}$$

$$K^{44}_{ij} = \int_0^l R_{44} \Psi'_i \Psi'_j dz \tag{33j}$$

The element stiffness matrix for the FOBT is given by:

$$K_{ij}^{11} = \int_0^l R_{11}\Psi_i'\Psi_j' dz \tag{34a}$$

$$K_{ij}^{12} = -\int_0^l R_{12}\Psi_i'\psi_j'' dz \tag{34b}$$

$$K_{ij}^{13} = 0 \tag{34c}$$

$$K_{ij}^{14} = \int_0^l R_{14}\Psi_i'\Psi_j' dz \tag{34d}$$

$$K_{ij}^{22} = \int_0^l R_{22}\psi_i''\psi_j'' dz \tag{34e}$$

$$K_{ij}^{23} = 0 \tag{34f}$$

$$K_{ij}^{24} = -\int_0^l R_{24}\psi_i''\Psi_j' dz \tag{34g}$$

$$K_{ij}^{33} = \int_0^l R_{55}\Psi_i'\Psi_j' dz \tag{34h}$$

$$K_{ij}^{34} = 0 \tag{34i}$$

$$K_{ij}^{44} = \int_0^l R_{44}\Psi_i'\Psi_j' dz \tag{34j}$$

The force vector is given by:

$$F_i^1 = \int_0^l \mathcal{P}_x\Psi_i dz \tag{35a}$$

$$F_i^2 = \int_0^l \mathcal{P}_z\Psi_i dz \tag{35b}$$

$$F_i^3 = \int_0^l \mathcal{P}_z\Psi_i dz \tag{35c}$$

$$F_i^4 = 0 \tag{35d}$$

11. References

References

[1] J. N. Reddy, Mechanics of laminated composite plates and shells: theory and analysis, CRC, 2004.

[2] Y. M. Ghugal, R. P. Shimpi, A review of refined shear deformation theories for isotropic and anisotropic laminated beams, Journal of Reinforced Plastics and Composites 20 (3) (2001) 255–272.

[3] R. Aguiar, F. Moleiro, C. M. Soares, Assessment of mixed and displacement-based models for static analysis of composite beams of different cross-sections, Composite Structures 94 (2) (2012) 601 – 616.

[4] W. Zhen, C. Wanji, An assessment of several displacement-based theories for the vibration and stability analysis of laminated composite and sandwich beams, Composite Structures 84 (4) (2008) 337 – 349.

[5] A. A. Khdeir, J. N. Reddy, Free vibration of cross-ply laminated beams with arbitrary boundary conditions, International Journal of Engineering Science 32 (12) (1994) 1971–1980.

[6] A. A. Khdeir, J. N. Reddy, Buckling of cross-ply laminated beams with arbitrary boundary conditions, Composite Structures 37 (1) (1997) 1–3.

[7] A. A. Khdeir, J. N. Reddy, An exact solution for the bending of thin and thick cross-ply laminated beams, Composite Structures 37 (2) (1997) 195–203.

[8] F.-G. Yuan, R. E. Miller, A higher order finite element for laminated beams, Composite Structures 14 (2) (1990) 125 – 150.

[9] H. Yu, A higher-order finite element for analysis of composite laminated structures, Composite Structures 28 (4) (1994) 375 – 383.

[10] G. Shi, K. Lam, T. Tay, On efficient finite element modeling of composite beams and plates using higher-order theories and an accurate composite beam element, Composite Structures 41 (2) (1998) 159 – 165.

[11] P. Subramanian, Flexural analysis of symmetric laminated composite beams using C1 finite element, Composite Structures 54 (1) (2001) 121 – 126.

[12] M. V. V. S. Murthy, D. R. Mahapatra, K. Badarinarayana, S. Gopalakrishnan, A refined higher order finite element for asymmetric composite beams, Composite Structures 67 (1) (2005) 27 – 35.

[13] K. H. Lo, R. M. Christensen, E. M. Wu, A high-order theory of plate deformationpart 2: Laminated plates, Journal of Applied mechanics 44 (1977) 669.

[14] T. Kant, A. Gupta, A finite element model for a higher-order shear-deformable beam theory, Journal of Sound and Vibration 125 (2) (1988) 193 – 202.

[15] T. Kant, B. S. Manjunatha, Higher-order theories for symmetric and unsymmetric fiber reinforced composite beams with C0 finite elements, Finite Elements in Analysis and Design 6 (4) (1990) 303 – 320.

[16] D. K. Maiti, P. Sinha, Bending and free vibration analysis of shear deformable laminated composite beams by finite element method, Composite Structures 29 (4) (1994) 421 – 431.

[17] R. U. Vinayak, G. Prathap, B. P. Naganarayana, Beam elements based on a higher order theory - I. Formulation and analysis of performance, Computers and Structures 58 (4) (1996) 775 – 789.

[18] A. M. Zenkour, Transverse shear and normal deformation theory for bending analysis of laminated and sandwich elastic beams., Mechanics of Composite Materials & Structures 6 (1999) 267 – 283.

[19] A. Catapano, G. Giunta, S. Belouettar, E. Carrera, Static analysis of laminated beams via a unified formulation, Composite Structures 94 (1) (2011) 75 – 83.

[20] E. Carrera, M. Petrolo, Refined one-dimensional formulations for laminated structure analysis, AIAA Journal 50 (2012) 176 – 189.

[21] M. Touratier, An efficient standard plate theory, International Journal of Engineering Science 29 (8) (1991) 901 – 916.

[22] K. P. Soldatos, A transverse shear deformation theory for homogeneous monoclinic plates, Acta mechanica 94 (3) (1992) 195–220.

[23] M. Karama, K. Afaq, S. Mistou, Mechanical behaviour of laminated composite beam by the new multi-layered laminated composite structures model with transverse shear stress continuity, International Journal of Solids and Structures 40 (6) (2003) 1525 – 1546.

[24] A. J. M. Ferreira, C. M. C. Roque, R. M. N. Jorge, Analysis of composite plates by trigonometric shear deformation theory and multiquadrics, Computers and Structures 83 (27) (2005) 2225 – 2237.

[25] M. Aydogdu, A new shear deformation theory for laminated composite plates, Composite Structures 89 (1) (2009) 94 – 101.

[26] J. Mantari, A. Oktem, C. G. Soares, Static and dynamic analysis of laminated composite and sandwich plates and shells by using a new higher-order shear deformation theory, Composite Structures, 84 (1) (2011) 37 – 49.

[27] J. N. Reddy, A simple higher-order theory for laminated composite plates, Journal of Applied Mechanics 51 (4) (1984) 745–752.

[28] R. M. Jones, Mechanics of Composite Materials, Taylor & Francis, 1999.

[29] W. B. Bickford, A consistent higher order beam theory, Developments in Theoretical and Applied Mechanics 11 (1982) 137150.

[30] P. Heyliger, J. Reddy, A higher order beam finite element for bending and vibration problems, Journal of Sound and Vibration 126 (2) (1988) 309 – 326.

[31] M. Eisenberger, An exact high order beam element, Computers & Structures 81 (3) (2003) 147 – 152.

[32] X. Lin, Y. Zhang, A novel one-dimensional two-node shear-flexible layered composite beam element, Finite Elements in Analysis and Design 47 (7) (2011) 676 – 682.

[33] J. F. Davalos, Y. Kim, E. J. Barbero, Analysis of laminated beams with a layer-wise constant shear theory, Composite Structures 28 (3) (1994) 241 – 253.

[34] K. Surana, S. Nguyen, Two-dimensional curved beam element with higher-order hierarchical transverse approximation for laminated composites, Computers & Structures 36 (3) (1990) 499 – 511.

[35] A. Chakraborty, D. R. Mahapatra, S. Gopalakrishnan, Finite element analysis of free vibration and wave propagation in asymmetric composite beams with structural discontinuities, Composite Structures 55 (1) (2002) 23 – 36.

Figure 1: Geometry of a laminated composite beam.

Figure 2: Configuration and cross section of a cantilever composite beam.

Figure 3: Distribution of stress σ_x through-the-thickness of a symmetric and an anti-symmetric cross-ply simply-supported composite beam with $L/h = 5$.

Figure 4: Distribution of stress σ_{xz} through-the-thickness of a symmetric and an anti-symmetric cross-ply simply-supported composite beam with $L/h = 5$.

Figure 5: Effect of shear deformation on symmetric cross-ply beam under a uniformly distributed load with cantilever and simply-supported boundary conditions.

Figure 6: Effect of shear deformation on anti-symmetric cross-ply beam under a uniformly distributed load with cantilever and simply-supported boundary conditions.

Figure 7: Variation of the bending and shear components of vertical displacements at mid-span with respect to the fiber angle change of a simply-supported composite beam with $L/h = 5$ under the uniformly distributed load.

Figure 8: Variation of the bending and shear components of vertical displacements at mid-span with respect to the fiber angle change of a simply supported composite beam with $L/h = 10$ under the uniformly distributed load.

Figure 9: Variation of the vertical displacement at mid-span with respect to the fiber angle change of simply supported composite beams with $L/h = 5$ and $L/h = 10$ under the uniformly distributed load.

Figure 10: Variation of the vertical displacement at mid-span with respect to the fiber angle change of cantilever composite beams with $L/h = 5$ and $L/h = 10$ under the concentrated tip load.

Figure 11: Variation of the axial displacement at free end with respect to the fiber angle change of cantilever composite beams with $L/h = 5$ and $L/h = 10$ under the concentrate load.

Figure 12: Variation of the angle of twist at free end with respect to the fiber angle change of cantilever composite beams with $L/h = 5$ and $L/h = 10$ under the concentrate load.

Table 1: Different transverse shear deformation functions.

Table 2: The maximum displacements of an isotropic cantilever beam and simply-supported beams.

Table 3: Material properties and loading case.

Table 4: Maximum displacement of a cantilever composite beam (mm).

Table 5: Non-dimensional mid-span displacements of a symmetric cross-ply beam under a uniformly distributed load with cantilever and simply supported boundary conditions.

Table 6: Non-dimensional mid-span displacements of an anti-symmetric cross-ply beam under a uniformly distributed load with cantilever and simply supported boundary conditions.

Table 7: Effect of span-to-height ratio on the non-dimensional stresses of a symmetric and an anti-symmetric cross-ply simply-supported composite beam.

CAPTIONS OF TABLES

Table 1. Different transverse shear deformation functions.
Table 2: The maximum displacements of an isotropic cantilever beam and simply-supported beam.
Table 3: Material properties and loading case.
Table 4: Maximum displacement of a cantilever composite beam (mm).
Table 5: Non-dimensional mid-span displacements of a symmetric cross-ply beam under a uniformly distributed load with cantilever and simply-supported boundary conditions.
Table 6: Non-dimensional mid-span displacements of an anti-symmetric cross-ply beam under a uniformly distributed load with cantilever and simply-supported boundary conditions.
Table 7: Effect of span-to-height ratio on the non-dimensional stresses of a symmetric and an anti-symmetric cross-plysimply-supportedcomposite beam.

Table 1. Different transverse shear deformation functions.

Theory	$f(z)$	$g(z)=1-f'(z)$
The Classical Beam Theory (CBT)	0	0
The First-order Beam Theory (FOBT)	0	1
The Higher-order Beam Theory (HOBT)	$z\left[\frac{4}{3}\left(\frac{z}{h}\right)^2\right]$	$\left[1-4\frac{z^2}{h^2}\right]$
The Sinusoidal Shear Beam Theory (SSBT)	$z-\frac{h}{\pi}\sin\left(\frac{\pi z}{h}\right)$	$\cos\left(\frac{\pi z}{h}\right)$

Table 2: The maximum displacements of an isotropic cantilever beam and simply-supported beam.

Theory	Reference	L=12	L=40	L=80	L=160
		h =12	h =12	h =12	h =12
a. Cantilever beam					
CBT	Euler theory [31]	0.013793	0.510855	4.0868	32.6948
	Present	0.013793	0.510860	4.0868	32.6950
FOBT	Timoshenko theory [31]	0.024552	0.546718	4.1586	32.8382
	Lin and Zhang [32]	0.024600	0.546700	4.1586	32.8380
	Present	0.024553	0.546720	4.1586	32.8380
HOBT	Murthy et al. [12]	0.023953	0.546119	4.1588	32.8376
	Heyliger and Reddy [30]	0.023931	0.545880	4.1567	32.8230
	Eisenberger [31]	0.023953	0.546119	4.1588	32.8376
	Present	0.023954	0.546120	4.1580	32.8380
SSBT	Present	0.023874	0.546000	4.1578	32.8370
Elasticity	Bickford [29]	0.024518	0.546680	4.1585	32.8380
b. Simplysupported beam					
CBT	Present	0.000647	0.079821	1.2771	20.4340
FOBT	Present	0.002261	0.097754	1.3489	20.7210
HOBT	Heyliger and Reddy [30]	0.002220	0.097703	1.3486	20.7170
	Present	0.002221	0.097714	1.3488	20.7210
SSBT	Present	0.002209	0.097679	1.3487	20.7210
Elasticity	Bickford [29]	0.002220	0.097712	1.3488	20.7210

Table 3: Material properties and loading case.

Material		Loading case	
Material 1	Material 2	Case A	Case B
$E_1/E_2 = 30$	$E_1/E_2 = 5$	$Q = 0$	$Q = 100$
$E_2 = 1.0\times10^6$	$E_2 = 1.0\times10^6$		
$G_{12}/E_2 = 0.5$	$G_{12}/E_2 = 0.5$	q =200	$q = 0$
$\nu_{12} = 0.25$	$\nu_{12} = 0.25$		

Table 4: Maximum displacement of a cantilever composite beam (mm).

Theory	Reference	Case A	Case B
CBT	Present	0.026285	0.4436
FOBT	Lin and Zhang [32]	0.030600	0.5410
	Davalos et al. [33]	0.030290	0.5520
	Present	0.030605	0.5408
HOBT	Surana and Nguyen [34]	0.030310	0.5350
	Present	0.030248	0.5305
SSBT	Present	0.030210	0.5295

Table 5: Non-dimensional mid-span displacements of a symmetric cross-ply beam under a uniformly distributed load with cantilever and simply-supported boundary conditions.

Theory	Reference	L/h			
		5	10	20	50
a. Cantilever beam					
CBT	Khdeir and Reddy [7]	2.198	2.198	2.198	2.198
	Present	2.203	2.203	2.203	2.203
FOBT	Khdeir and Reddy [7]	6.698	3.323	-	2.243
	Chakraborty et al. [35]	6.693	3.321	-	2.242
	Present	6.703	3.328	2.485	2.248
HOBT	Khdeir and Reddy [7]	6.824	3.455	-	2.251
	Murthy et al. [12]	6.836	3.466	-	2.262
	Present	6.830	3.461	2.530	2.257
SSBT	Present	6.842	3.478	2.536	2.258
b. Simplysupported beam					
CBT	Aguiar et al. [3]	0.646	0.646	0.646	0.646
	Khdeir and Reddy [7]	0.646	0.646	0.646	0.646
	Present	0.648	0.648	0.648	0.648
FOBT	Aguiar et al. [3]	2.146	1.021	0.740	0.661
	Khdeir and Reddy [7]	2.146	1.021	-	0.661
	Chakraborty et al. [35]	2.145	1.020	-	0.660
	Present	2.148	1.023	0.742	0.663
HOBT	Aguiar et al. [3]	2.426	1.105	0.762	0.665
	Khdeir and Reddy [7]	2.412	1.096	-	0.665
	Murthy et al. [12]	2.398	1.090	-	0.661
	Zenkour [18]	2.414	1.098	-	0.666
	Present	2.414	1.098	0.761	0.666
SSBT	Present	2.444	1.108	0.764	0.667

Table 6: Non-dimensional mid-span displacements of an anti-symmetric cross-ply beam under a uniformly distributed load with cantilever and simply-supported boundary conditions.

Theory	Reference	L/h			
		5	10	20	50
a. Cantilever beam					
CBT	Khdeir and Reddy [7]	11.293	11.293	11.293	11.293
	Present	11.319	11.319	11.319	11.319
FOBT	Khdeir and Reddy [7]	16.436	12.579	-	11.345
	Chakraborty et al. [35]	16.496	12.579	-	11.345
	Present	16.461	12.604	11.640	11.370
HOBT	Khdeir and Reddy [7]	15.279	12.343	-	11.337
	Murthy et al. [12]	15.334	12.398	-	11.392
	Present	15.305	12.369	11.588	11.363
SSBT	Present	15.173	12.340	11.582	11.362
b. Simply-supported beam					
CBT	Khdeir and Reddy [7]	3.322	3.322	3.322	3.322
	Present	3.329	3.329	3.329	3.329
FOBT	Khdeir and Reddy [7]	5.036	3.750	-	3.339
	Chakraborty et al. [35]	5.048	3.751	-	3.353
	Present	5.043	3.757	3.436	3.346
HOBT	Khdeir and Reddy [7]	4.777	3.688	-	3.336
	Murthy et al. [12]	4.750	3.668	-	3.318
	Zenkour [18]	4.788	3.697	-	3.344
	Present	4.785	3.696	3.421	3.344
SSBT	Present	4.749	3.687	3.419	3.343

Table 7: Effect of span-to-height ratio on the non-dimensional stresses of a symmetric and an anti-symmetric cross-ply simply-supportedcomposite beam.

Lay-ups	Theory	Reference	σ_x			σ_{xz}		
			L/h = 5	L/h=10	L/h=20	L/h=5	L/h=10	L/h=20
$[0^0/90^0/0^0]$	CLT	Zenkour [18]	0.7776	0.7776	-	-	-	-
		Present	0.7780	0.7780	0.7780	-	-	-
	FOBT	Zenkour[18]	0.7776	0.7776	-	0.2994	0.2994	0.2994
		Present	0.7780	0.7780	0.7780	0.2925	0.2925	0.2925
	HOBT	Zenkour[18]	1.0669	0.8500	-	0.4057	0.4311	-
		Present	1.0670	0.8503	0.7961	0.4057	0.4311	0.4438
	SSBT	Present	1.0920	0.8566	0.7976	0.4233	0.4533	0.4683
$[0^0/90^0]$	CLT	Zenkour[18]	0.2336	0.2336	-	-	-	-
		Present	0.2335	0.2335	0.2335	-	-	-
	FOBT	Zenkour[18]	0.2336	0.2336	-	0.8553	0.8553	-
		Present	0.2335	0.2335	0.2335	0.8357	0.8357	0.8357
	HOBT	Zenkour[18]	0.2362	0.2343	-	0.9211	0.9572	-
		Present	0.2361	0.2342	0.2337	0.9187	0.9484	0.9425
	SSBT	Present	0.2357	0.2341	0.2337	0.9308	0.9653	0.9624

CAPTIONS OF FIGURES

Figure 1: Geometry of a laminated composite beam.

Figure 2: Configuration and cross section of a cantilever composite beam.

Figure 3: Distribution of stress σ_x through-the-thickness of a symmetric and an anti-symmetric cross-ply simply-supported composite beam with L/h =5.

Figure 4: Distribution of stress σ_{xz} through-the-thickness of a symmetric and an anti-symmetric cross-ply simply-supported composite beam with L/h = 5.

Figure 5: Effect of shear deformation on symmetric cross-ply beam under a uniformly distributed load with cantilever and simply-supported boundary conditions.

Figure 6: Effect of shear deformation on anti-symmetric cross-ply beam under a uniformly distributed load with cantilever and simply-supported boundary conditions.

Figure 7: Variation of the bending and shear components of vertical displacements at mid-span with respect to the fiber angle change of a simply-supported composite beam with L/h = 5 under the uniformly distributed load.

Figure 8: Variation of the bending and shear components of vertical displacements at mid-span with respect to the fiber angle change of a simply-supported composite beam with L/h = 10 under the uniformly distributed load.

Figure 9: Variation of the vertical displacements at mid-span with respect to the fiber angle change of simply-supported composite beams with L/h = 5 and L/h = 10 under the uniformly distributed load.

Figure 10: Variation of the vertical displacement at free end with respect to the fiber angle change of cantilever composite beams with L/h = 5 and L/h = 10 under the concentrate load.

Figure 11: Variation of the axial displacement at free end with respect to the fiber angle change of cantilever composite beams with L/h = 5 and L/h = 10 under the concentrate load.

Figure 12: Variation of the angle of twist at free end with respect to the fiber angle change of cantilever composite beams with L/h = 5 and L/h = 10 under the concentrate load.

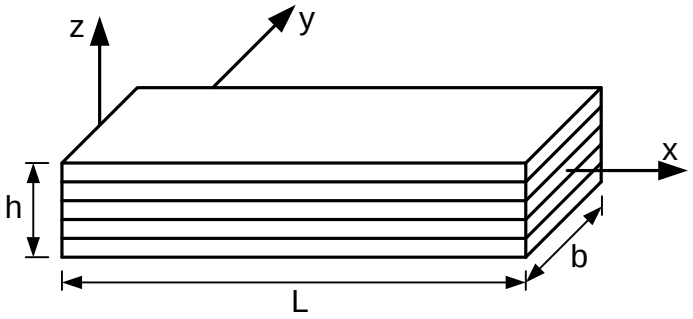

Figure 1: Geometry of a laminated composite beam.

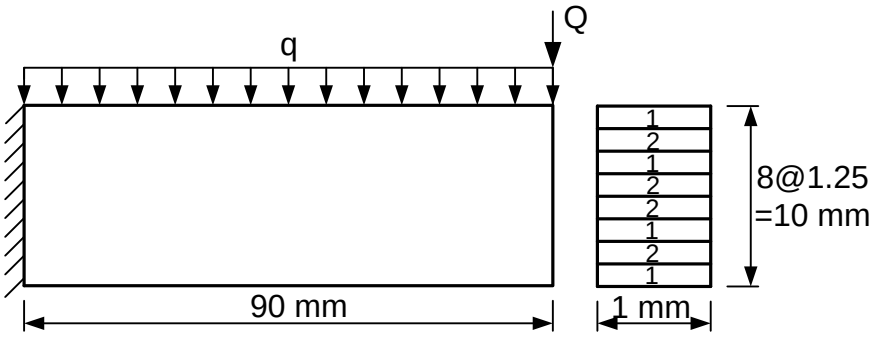

Figure 2: Configuration and cross section of a cantilever composite beam.

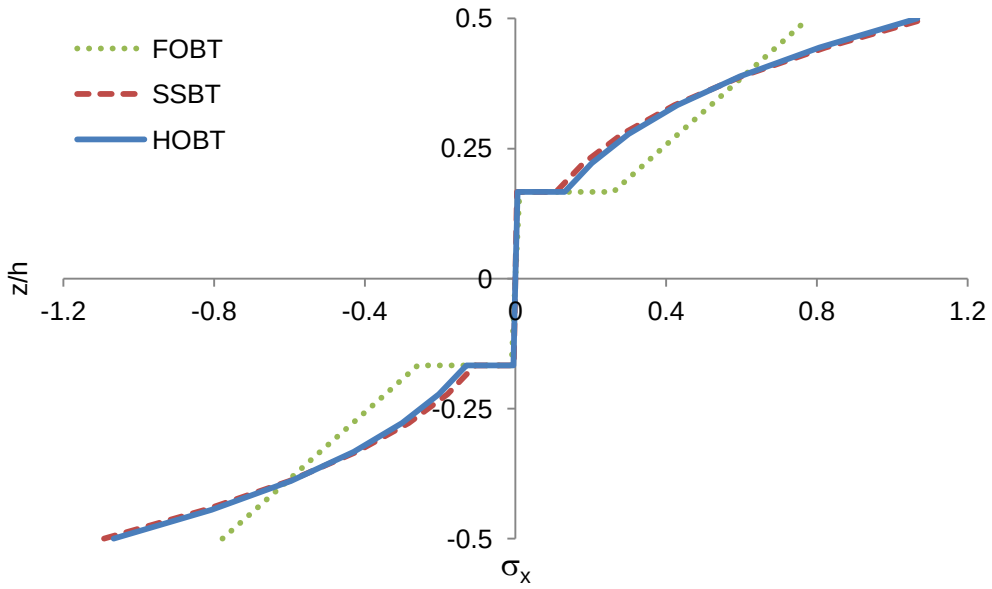

a. Symmetric cross-ply.

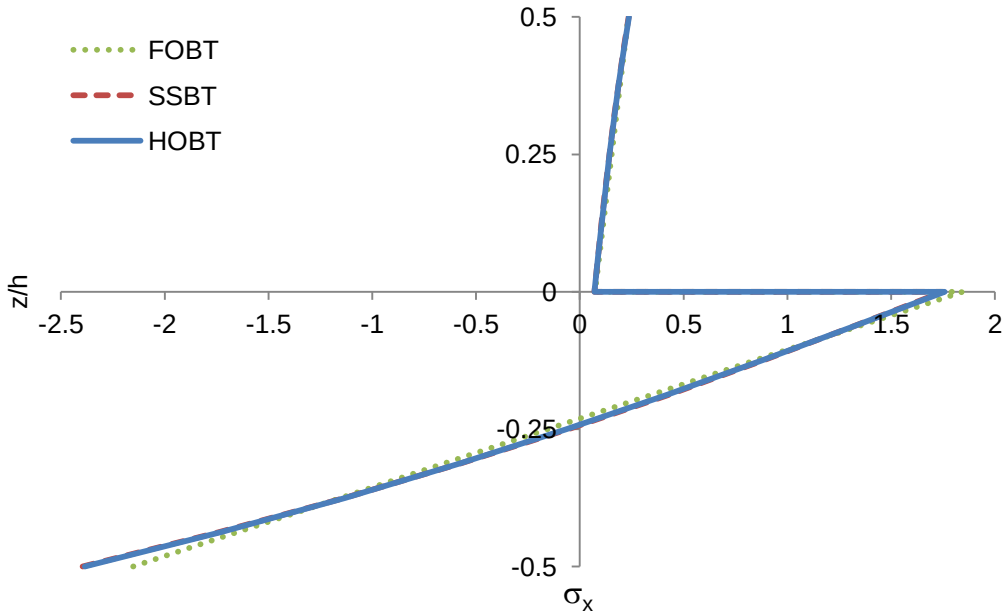

b. Anti-symmetric cross-ply.

Figure 3: Distribution of stress σ_x through-the-thickness of a symmetric and an anti-symmetric cross-ply simply-supported composite beam with L/h =5.

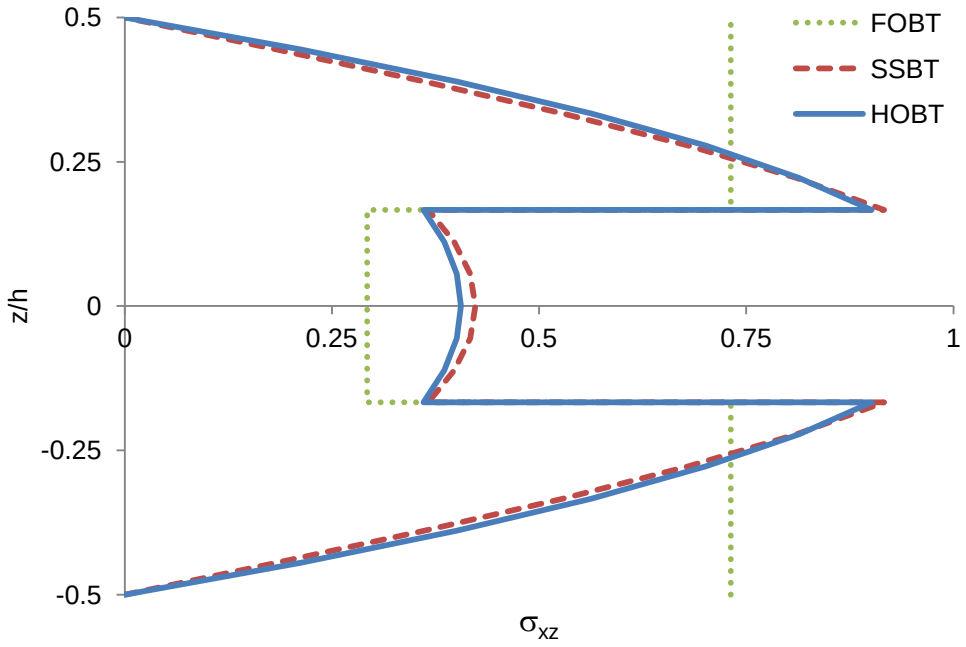

a. Symmetric cross-ply

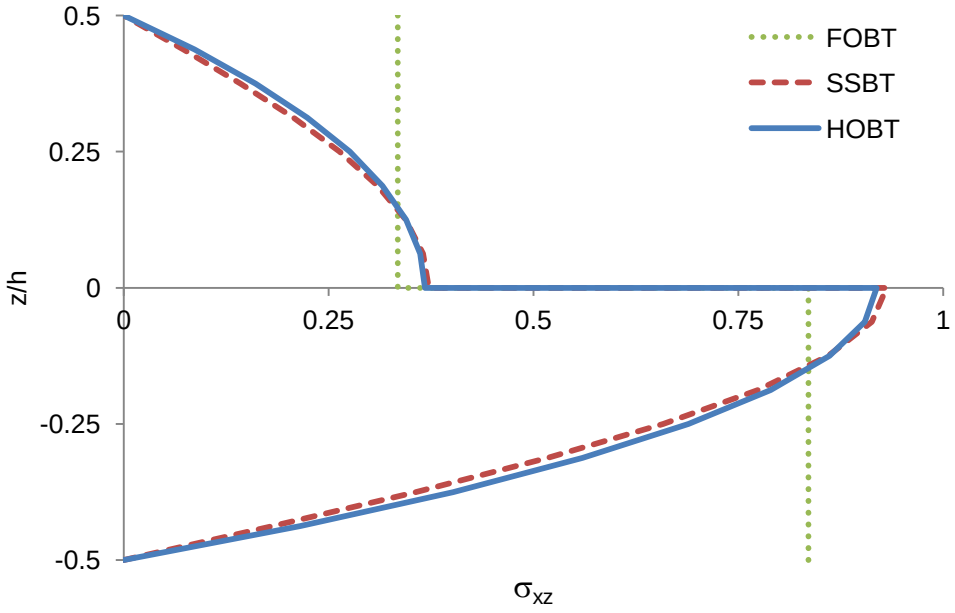

b. Anti-symmetric cross-ply

Figure 4: Distribution of stress σ_{xz} through-the-thickness of a symmetric and an anti-symmetric cross-ply simply-supported composite beam with L/h = 5.

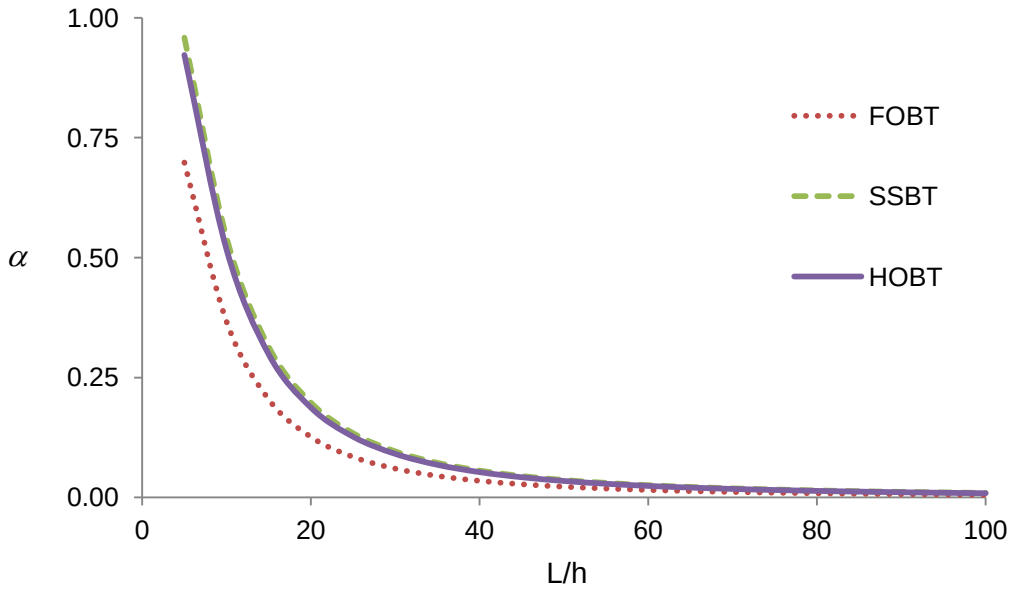

a. Cantilever beam

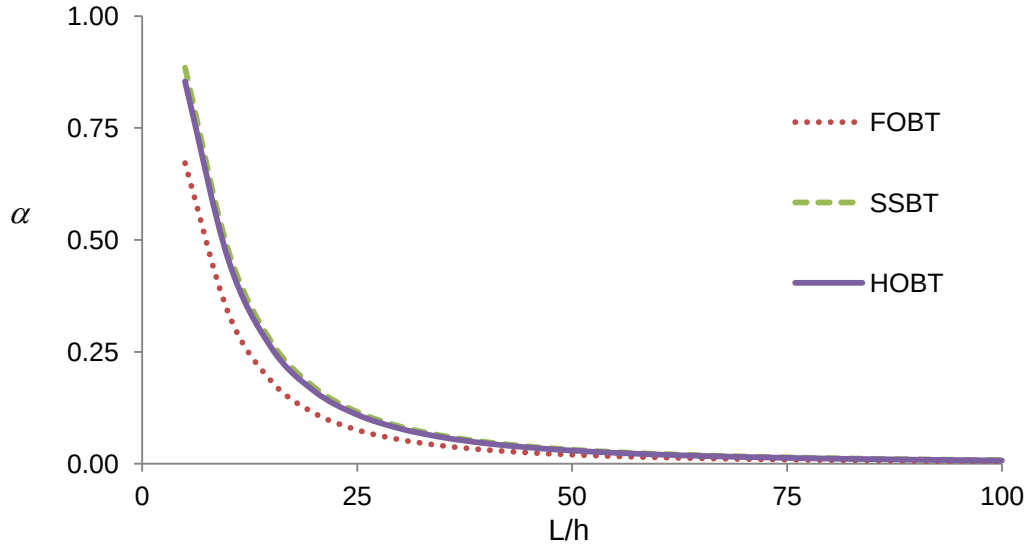

b. Simply-supported beam

Figure 5: Effect of shear deformation on symmetric cross-ply beam under a uniformly distributed load with cantilever and simply-supported boundary conditions.

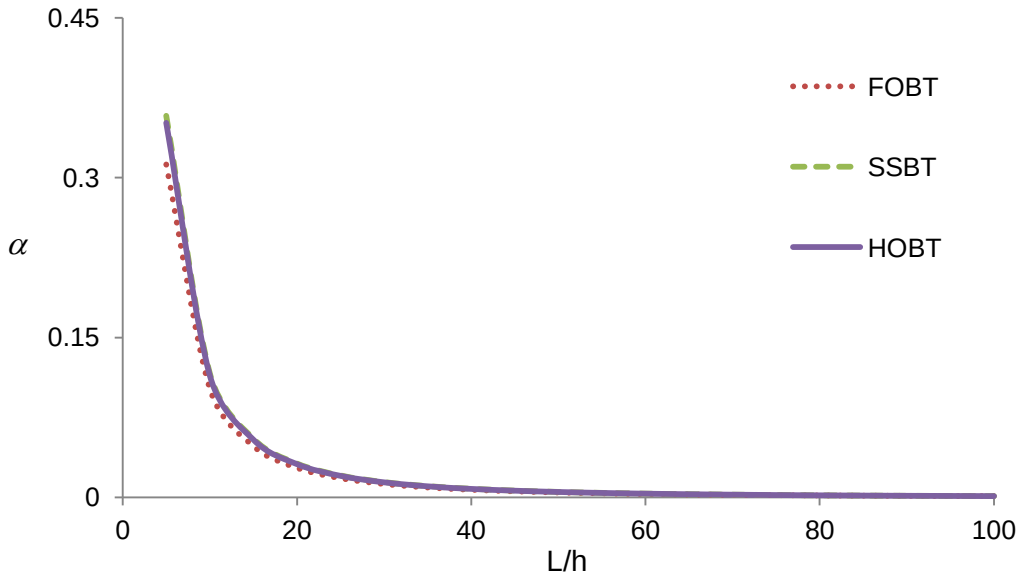

a. Cantilever beam

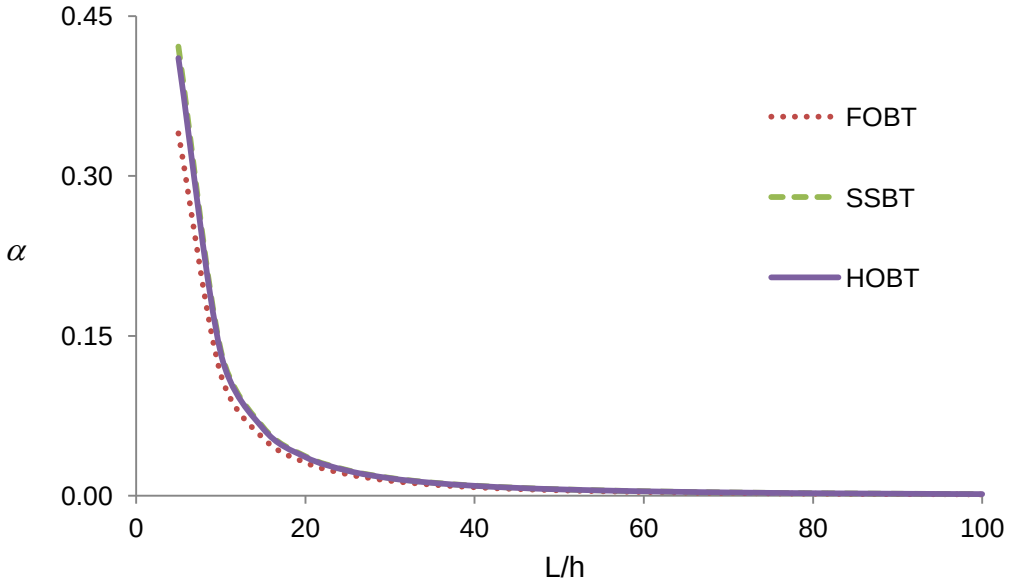

b. Simply-supported beam

Figure 6: Effect of shear deformation on anti-symmetric cross-ply beam under a uniformly distributed load with cantilever and simply-supported boundary conditions.

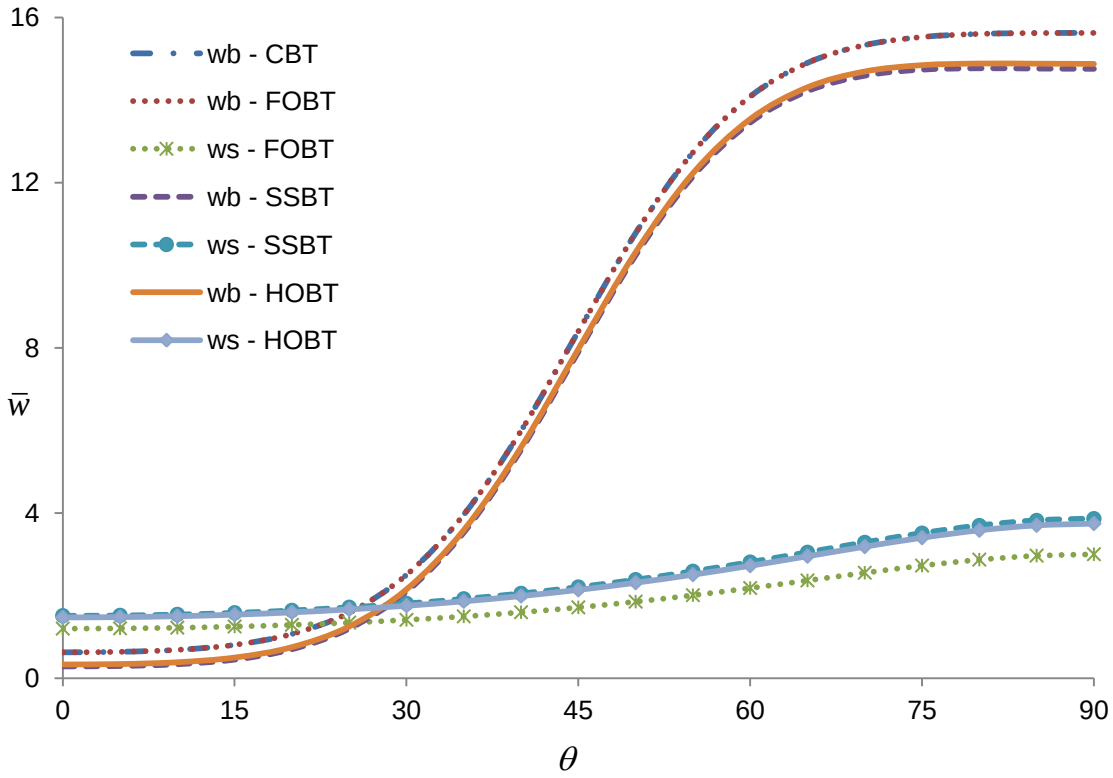

Figure 7: Variation of the bending and shear components of vertical displacements at mid-span with respect to the fiber angle change of a simply-supported composite beam with L/h = 5 under the uniformly distributed load.

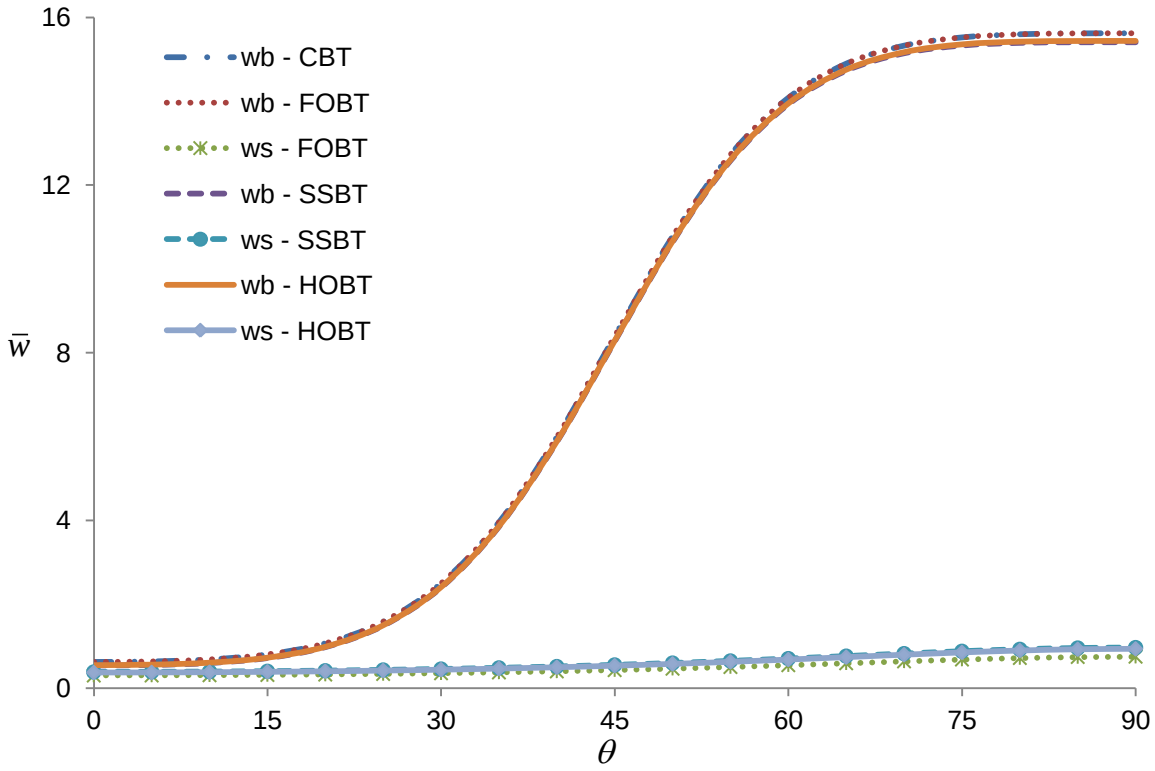

Figure 8: Variation of the bending and shear components of vertical displacements at mid-span with respect to the fiber angle change of a simply-supported composite beam with L/h = 10 under the uniformly distributed load.

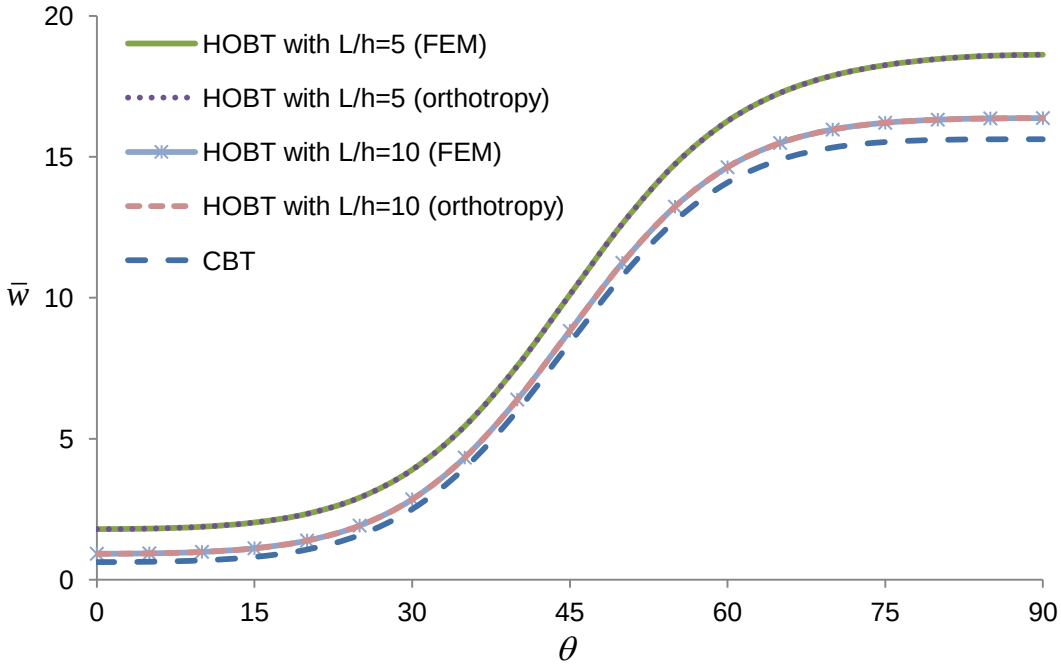

Figure 9: Variation of the vertical displacements at mid-span with respect to the fiber angle change of simply-supported composite beams with L/h = 5 and L/h = 10 under the uniformly distributed load.

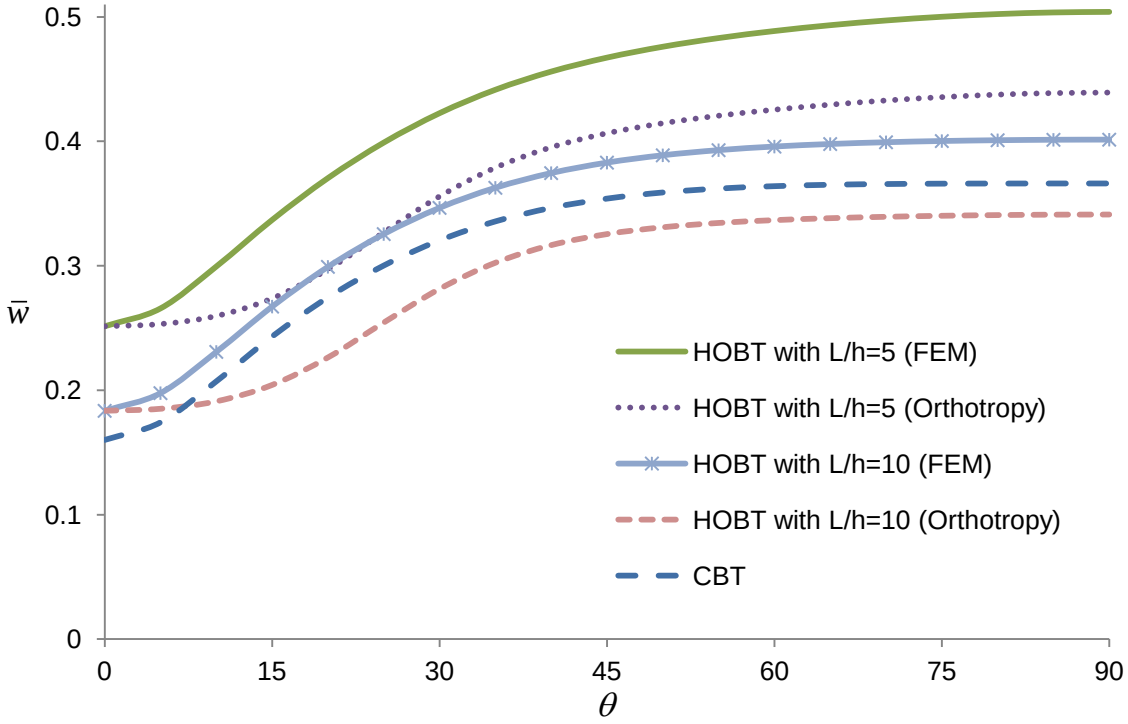

Figure 10: Variation of the vertical displacement at free end with respect to the fiber angle change of cantilever composite beams with L/h = 5 and L/h = 10 under the concentrate load.

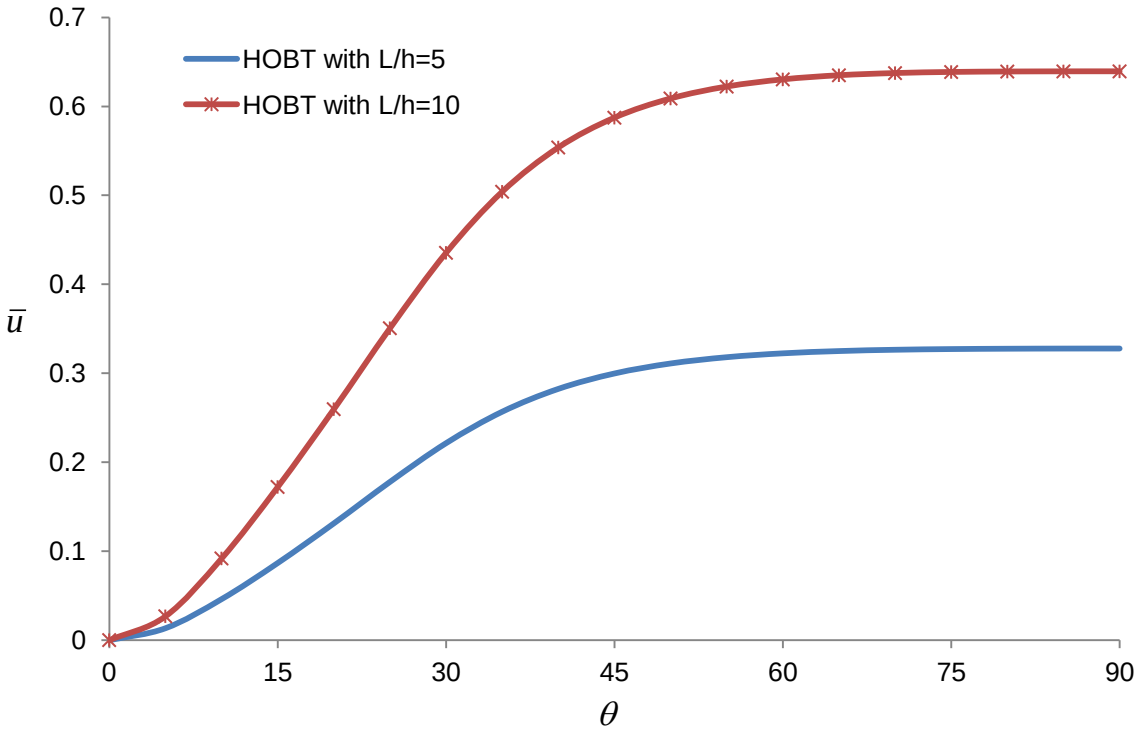

Figure 11: Variation of the axial displacement at free end with respect to the fiber angle change of cantilever composite beams with L/h = 5 and L/h = 10 under the concentrate load.

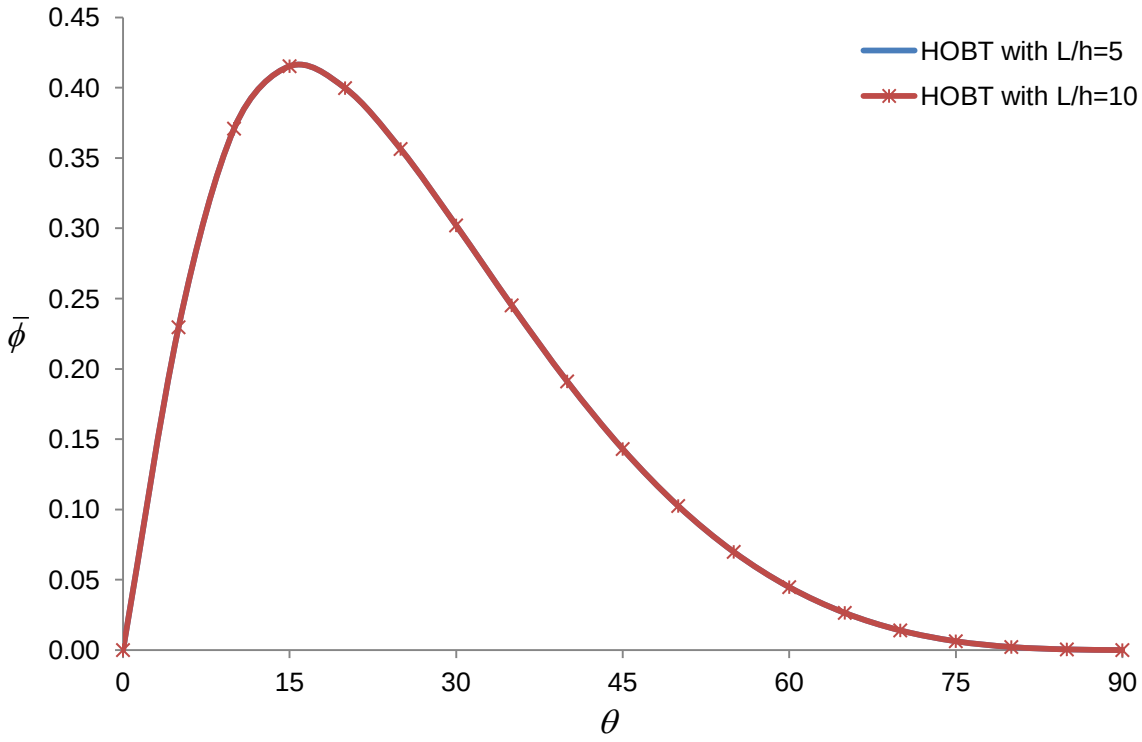

Figure 12: Variation of the angle of twist at free end with respect to the fiber angle change of cantilever composite beams with L/h = 5 and L/h = 10 under the concentrate load.